

# Phase-sensitive time-domain terahertz reflection spectroscopy

A. Pashkin,<sup>a)</sup> M. Kempa, H. Němec, F. Kadlec, and P. Kužel

*Institute of Physics, Academy of Sciences of the Czech Republic and Center for Complex Molecular Systems and Biomolecules, Na Slovance 2, 182 21 Prague 8, Czech Republic*

(Received 1 April 2003; accepted 1 August 2003)

An approach to time-domain terahertz reflection spectroscopy is proposed and demonstrated. It allows one to obtain very accurately the relative phase of a reflected THz wave form, and consequently the complex dielectric function can be precisely extracted. The relevant setup was demonstrated to allow measurements of a variety of samples: we present results for doped silicon and for ferroelectric SrBi<sub>2</sub>Ta<sub>2</sub>O<sub>9</sub> (bulk ceramics as well as thin film on sapphire substrates).

© 2003 American Institute of Physics. [DOI: 10.1063/1.1614878]

## I. INTRODUCTION

Time-domain terahertz transmission spectroscopy (TDTTS) has become a standard method for measurements of complex dielectric constant or conductivity of dielectrics, semiconductors, and superconductors in the millimeter and submillimeter spectral range.<sup>1</sup> The technique requires measurement of the temporal profile of the electric field of a picosecond terahertz (THz) pulse transmitted through an investigated sample. The complex spectrum of this pulse is normalized by a reference spectrum (obtained when the sample is removed from the THz beam path) thus yielding the complex transmittance of the sample. Finally, the complex refractive index in the whole frequency range studied is obtained through numerical solution of a system of two real nonlinear equations for the transmittance.<sup>2</sup> Let us emphasize the importance of the reference measurement: it ensures the result is independent of the THz pulse shape as well as of instrumental functions.

The transmission setup is fully developed and reliable, but it can be applied only to transparent samples. However, in the case of samples that are opaque in the THz frequency range (thick and/or with high dielectric loss), the transmission geometry is not useful and the use of time-domain THz reflection spectroscopy (TDTRS) is required. Furthermore, in the case of thin films on thick substrates, TDTTS sometimes does not offer sufficient sensitivity to provide precise information about the optical constants of a thin film. This is due to a large difference between the phase change of the THz signal induced by the thin film and that related to the substrate.<sup>3</sup> Thus the evaluation of transmittance related to the thin film involves large errors. In this case, TDTRS can provide valuable information about such structures because the radiation reflected on air–thin film–substrate interfaces is independent of the substrate thickness.

TDTRS as a spectroscopic method, and in analogy with TDTTS, requires also a reference measurement which can be obtained, e.g., using the reflection on a mirror with known characteristics. The main difficulty in realization of TDTRS then consists of correct determination of the reflectance

phase which is strongly affected by errors in the relative position of the sample and reference mirror.<sup>4–9</sup> Due to the very strong dependence of the dielectric function on the reflectance phase, mispositioning as small as 1  $\mu\text{m}$  can significantly influence the dielectric function calculated.<sup>10</sup>

In this article we present a new approach to TDTRS designed to provide in many cases easy and accurate measurement of the phase of complex reflectance. We have tested our setup using different types of samples which were chosen to illustrate potential application of the method. The THz spectral range is appropriate for measurement of the carrier scattering rate and plasma frequency of doped semiconductors. The first samples studied were thus two *n*-type silicon wafers with different levels of doping. The next sample was a ferroelectric ceramic, SrBi<sub>2</sub>Ta<sub>2</sub>O<sub>9</sub> (SBT), which is a very good candidate for nonvolatile ferroelectric memories due to its polarization fatigue-free nature and low switching voltage.<sup>11</sup> It presents a rather strong IR-active soft phonon mode in the frequency range studied and therefore it cannot be investigated by TDTTS. The last sample was a thin film of the same compound deposited on a sapphire substrate; this structure allows direct comparison of the reflection and transmission measurements.

## II. OVERVIEW OF THE PHASE PROBLEM

Because THz radiation is reflected directly onto the sample surface, the phase shift induced by the sample is much smaller than that in the transmission experiment where it is proportional to the sample thickness. Therefore even small errors in phase lead to appreciable errors in determination of the complex refractive index. This is demonstrated in Fig. 1. The curves in the plane of the complex refractive index correspond to constant values of the reflectance amplitude and adjacent points correspond to the difference in reflectance phase induced by a 1  $\mu\text{m}$  shift of the sample for frequency of 1 THz. The shape of the curve remains unchanged for other frequencies while the spacing between the points is proportional to the frequency. For a low absorption index (close to the real axis) the slope of the curves is almost vertical. Therefore a small phase error leads to large errors in the calculated absorption index. On the other hand, when the

<sup>a)</sup>Electronic mail: pashkin@fzu.cz

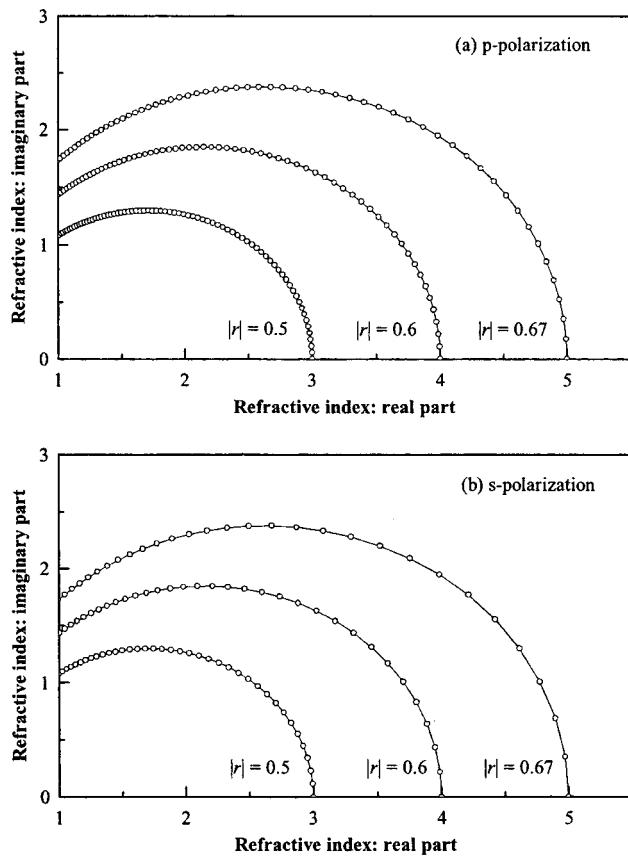


FIG. 1. Complex refractive indices corresponding to the same reflectance amplitude of (a) *p*- and (b) *s*-polarized waves. Adjacent points correspond to phase change equivalent to  $1\ \mu\text{m}$  displacement of the sample. The values are calculated for angle of incidence of  $45^\circ$  and frequency of 1 THz.

refractive and absorption indices are comparable, the slope is horizontal and errors in the real part of the refractive index become dominant. One can also note that the points are more dense in the case of *p* polarization, which implies better stability with respect to phase errors compared to the case of *s* polarization.

To avoid the problem of phase uncertainty in TDTRS, several different approaches have been used. One of them consists of substitution of the reference signal by a signal reflected from the sample under specific conditions. Howells and Schlie<sup>4</sup> have investigated the low-temperature dielectric function of undoped InSb in this way taking as a reference the wave form obtained at 360 K. They used the fact that the reflectance of InSb at high temperature is comparable to that of a silver mirror due to the narrow band gap of the material. Thrane *et al.*<sup>5</sup> have measured the refractive index of liquid water in a silicon cell using the signal reflected from the air–silicon interface as a reference and the signal from the silicon–water interface as a sample wave form. Such methods make use of specific sample properties and can be applied only in particular cases. Other methods similar to ellipsometry extract the complex dielectric function from the *s*- and *p*-polarized THz signals reflected from the sample at high angles of incidence.<sup>6,7</sup> This approach provides very satisfactory results in some cases. On the other hand, it requires good quality THz polarizers and, for highly reflective

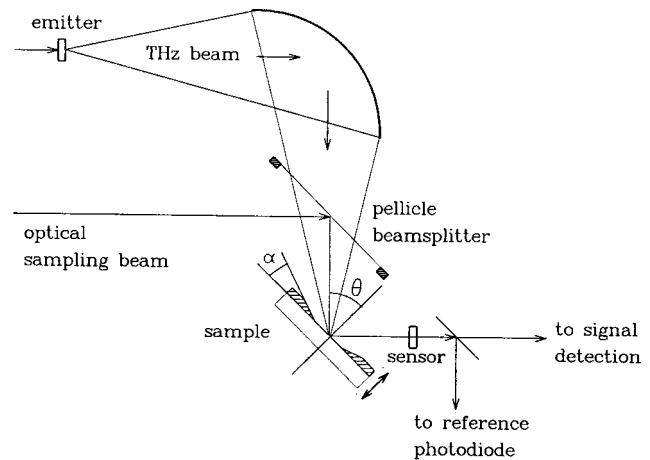


FIG. 2. Schematic of the TDTRS experimental setup (see the text for details).

samples, it is necessary to measure under angles of incidence close to  $90^\circ$ , which restricts the measurements to only large enough homogeneous samples. In the case of TDTRS with a reference mirror, the uncontrollable time shift of the reference pulse can be *a posteriori* adjusted to fit some model of the dielectric response<sup>8</sup> or to minimize the difference between the measured and calculated interference pattern in a silicon slab attached to the sample surface.<sup>10</sup> The last method does not make any assumption about the sample dielectric behavior model, but is rather difficult to realize because there should be good optical contact between the sample and the slab. Recently Hashimshony *et al.*<sup>9</sup> have succeeded in performing TDTRS measurements of epitaxial semiconductor layers using a special sample holder which allowed replacing the reference mirror by the sample within accuracy of  $1\ \mu\text{m}$ . However, this is not an easy task, and in some cases even this precision is not sufficient for correct determination of the dielectric function.

### III. EXPERIMENTAL SETUP

Figure 2 shows schematically the relevant part of our experimental setup. THz pulses are emitted by a ZnTe [011] crystal via optical rectification of amplified femtosecond laser pulses (wavelength 800 nm, repetition rate 1 kHz) and focused onto the sample (or reference mirror) by an ellipsoidal mirror. The optical sampling pulses have a variable time delay with respect to THz pulses and serve as electro-optic detector for the THz wave form. The key idea consists of making the two beams coincide between the emitter and the sample, in contrast to the usual arrangement where there is coincidence between the sample and the sensor. In our geometry both beams propagate collinearly and reflect from the sample surface. The sample leans on a flat surface of a circular metallic aperture at angle  $\theta$  with respect to the incident beam. The aperture angle  $\alpha$  has to be small enough ( $\alpha < 45^\circ - \theta/2$ ) to ensure that possible weak reflection of the THz beam off the aperture falls away from the sensor. To maximize a clear aperture for the THz beam,  $\theta$  should be kept small, however, in practice,  $\theta$  needs to be larger than about  $10^\circ$ . In this article we present results obtained for angles of incidence  $\theta = 12.5^\circ$  and  $45^\circ$ . This latter geometry (depicted in

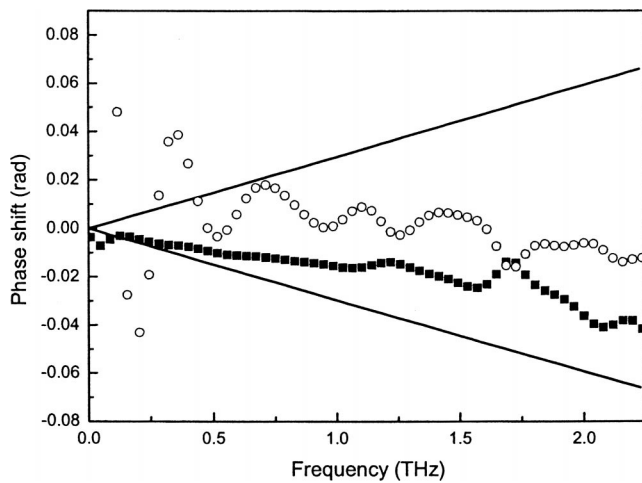


FIG. 3. Measured phase difference introduced by 10  $\mu\text{m}$  (closed squares) and 1 mm (open circles) shifts of the reference mirror in the setup in Fig. 2 with  $\theta=45^\circ$  and  $p$  polarization. The classical setup, where only the THz beam reflects off the sample, requires the sample surface to be positioned within 1  $\mu\text{m}$  of the reference mirror surface in order to fit the phase inside the area between the solid lines.

Fig. 2) is of particular interest since it is suitable for measurements in standard cryostats with perpendicular windows. The signal reflected is detected using the electro-optic effect by a ZnTe [011] sensor which is placed directly after the sample. Measured THz wave forms are normalized by the voltage on a reference photodiode which is proportional to the intensity of the sampling beam. In this way, the difference in optical reflectance between the reference mirror and the sample is taken into account. Most measurements were performed using  $p$ -polarized THz pulses, however, a reflectivity experiment with  $s$ -polarized radiation has been also tested.

Our arrangement is based on the setup used by Li *et al.*<sup>12</sup> who took advantage of the possibility to easily change the incidence angle to perform TDTRS of a thin film near the Brewster angle. In our setup, a fixed angle of incidence and reflection is used and the focusing mirror after the sample is absent. We benefit from the major feature that displacement of the sample changes the length of the optical path by precisely the same amount for both beams, and produces no phase change in the measured THz wave form. To illustrate this, we have performed measurements of the THz signal for different positions of a gold mirror, shifting it in the way shown by the bold arrow in Fig. 2. It has been found that even a 1 mm shift from the initial position in both directions does not change the THz wave form. Figure 3 shows the phase differences between THz pulses measured with the mirror shifted 10  $\mu\text{m}$  and 1 mm. It can be seen in Fig. 3 that the phase error does not depend on the mirror shift. The limiting factor for phase reproducibility is then the temporal stability of the whole setup (including the beam-pointing stability of the laser source) rather than precise positioning of the sample. Similarly, the setup described is not sensitive to errors in the relative angular alignment of the sample and reference mirror. The absence of a focusing mirror after the sample allows us to avoid problems due to, e.g., possible lower optical quality of the mirror surface or deviation of its

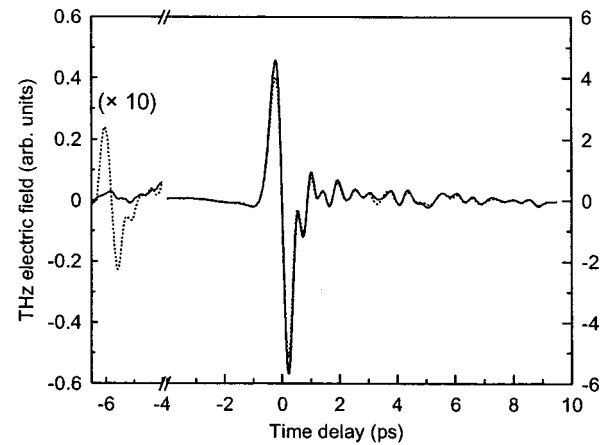


FIG. 4. THz wave forms obtained in the reflection setup for SBT thin film on a sapphire substrate. Solid line: Sample with a blackened rear surface; dotted line: sample without this treatment. The replica near  $-6$  ps indicates the presence of the sampling beam reflection at the rear surface. The difference in amplitude of the main pulses (near 0 ps delay) is due to the change in sampling beam intensity and indicates the extent of error that would result of the parasite reflection were not removed.

shape from the ideal one. In fact, focusing of the THz beam onto the sensor is not necessary since standard THz experiments offer a very good signal-to-noise ratio nowadays.

Suitable samples for measurement have to fulfill the following requirements: (i) have an optically flat surface to allow nondiffusive (specular) reflection of the sampling beam and (ii) the absence of secondary reflections of the sampling beam from the rear of the sample. According to our experience, the majority of crystalline and ceramics samples can be polished with sufficient precision to satisfy the former condition. The latter one is critical for optically transparent samples where an echo of the sampling beam reflected from the back side of the sample adds a systematic error to the reference photodiode voltage and is responsible for several replicas of the THz pulse in the measured wave form. Parasite reflections can be unambiguously detected through a replica that occurs at time  $\Delta t$  before the main THz pulse:

$$\Delta t = \frac{2n^2 d}{c\sqrt{n^2 - \sin^2 \theta}}, \quad (1)$$

where  $n$  is the optical refractive index of the sample and  $d$  its thickness (see Fig. 4).

This situation particularly occurs in thin films deposited on optically transparent substrates or in dielectric single crystals. In these cases, special precautions have to be taken: (i) roughening or blackening of the back surface of the sample; (ii) spatial filtering of the sampling beam after the sensor.

## IV. RESULTS AND DISCUSSION

### A. Doped silicon

Moderately or highly doped silicon crystals are of particular interest as test samples for the TDTRS.<sup>8,10</sup> They have noticeable dispersion of the complex conductivity in the THz frequency range and knowledge of their dc conductivity provides a good possibility to verify the model fits of TDTRS

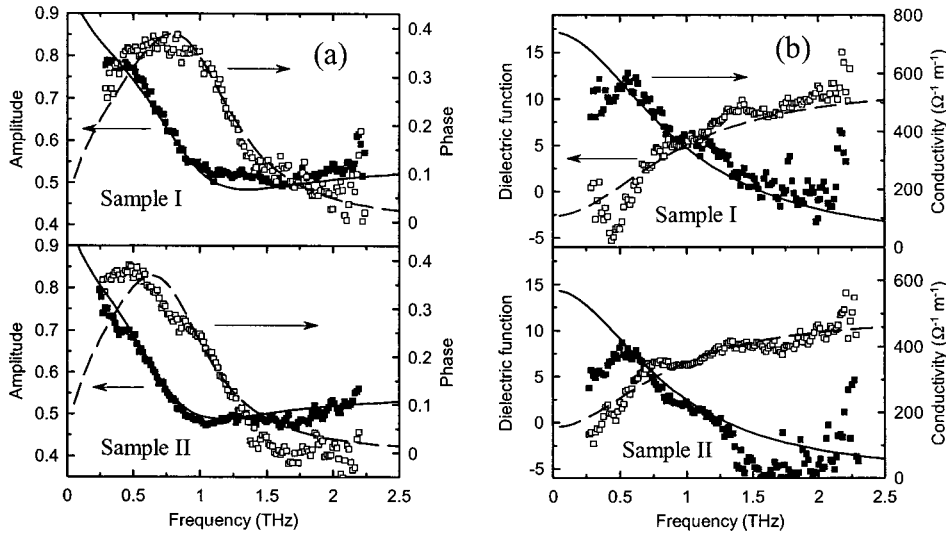


FIG. 5. (a) Complex reflectance at  $\theta=12.5^\circ$ ,  $p$  polarization and (b) dielectric function and conductivity of doped silicon samples. Points: Experimental data; lines: fits using the Drude model.

spectra. Our experimental arrangement requires the optical sampling beam to reflect from the sample surface which seems to be undesirable for measurements of semiconductors, because of photoexcitation of additional carriers in the sample. It means that the density of photocarriers should be always carefully estimated during evaluation of these experiments. Taking into account the sampling beam cross section (approximately  $0.5 \text{ mm}^2$ ), optical absorption length in silicon ( $10 \mu\text{m}$  at  $800 \text{ nm}$ ), and sampling pulse energy ( $0.5 \text{ nJ}$ ) we obtain photocarrier density  $n_0 \approx 2 \times 10^{14} \text{ cm}^{-3}$  which is two orders of magnitude smaller than the impurity concentration in our samples. If the photocarriers are long lived, which is the case for silicon, the laser repetition rate should be taken into account. Let us consider a sequence of pulses with the time separation  $T$  ( $1 \text{ ms}$  in our case); then the density of carriers can be found from the following relation:

$$n(t) = n_0 e^{-(t/\tau)} + n_0 e^{-(t+T/\tau)} + n_0 e^{-(t+2T/\tau)} + \dots$$

$$= \frac{n_0 e^{-(t/\tau)}}{1 - e^{-(T/\tau)}}, \quad (2)$$

where  $\tau$  is the carrier lifetime. Here we neglect the diffusion process which additionally decreases the carrier density. If  $T > \tau \ln 2$  (which is the case for moderately and highly doped silicon where  $\tau$  is smaller than  $1 \text{ ms}$ ), then  $n(t)$  is increased compared to the carrier density created by a single sampling pulse by a factor smaller than 2. Therefore the influence of the sampling beam can be neglected for our experimental conditions.

In the case of direct gap semiconductors (GaAs, InP, etc.), the absorption length is smaller than in indirect semiconductors such as silicon and  $n_0$  can be higher by an order of magnitude or more. However, due to the direct character of the band gap, the probability of carrier recombination is also higher, so the carrier lifetime  $\tau$  is appreciably smaller and possibly  $\tau \ll T$ . One can take advantage of this to adopt the experimental approach described below. The excess carrier density in the sample just before the arrival of the next sampling pulse  $n(T)$  becomes much smaller than  $n_0$ :

$$n(T) = \frac{n_0}{e^{T/\tau} - 1}. \quad (3)$$

To achieve a THz pulse that reflects off the sample in such conditions, it is sufficient to introduce an appropriate small delay between the THz and sampling pulses after their reflection from the sample in order to make the optical path of the THz beam between the sample and the sensor longer than that of the sampling beam. Then, the detection system processes information about the THz field unaffected by the photoexcitation, since it reflects from the sample surface before the sampling pulse. For this one can insert, e.g., a (0001) sapphire slab just before the sensor (sapphire is transparent to both optical and THz radiation and induces a pulse walkoff of  $4.5 \text{ ps/mm}$ ). In order to test this approach we have put a  $0.5 \text{ mm}$  thick sapphire plate into optical contact with the ZnTe sensor and we have significantly increased the sampling pulse energy (up to  $5 \text{ nJ}$ ). No change in reflectance spectra has been observed compared to those obtained with  $0.5 \text{ nJ}$  pulse energy.

We present here a measurement of complex reflectance spectra of two  $n$ -type phosphorus doped silicon wafers supplied by ON Semiconductor-Terosil, Rožnov pod Radhoštěm, with specifications  $\rho_{\text{dc}} = 0.128 \Omega \text{ cm}$  (sample I) and  $\rho_{\text{dc}} = 0.153 \Omega \text{ cm}$  (sample II) with possible deviations less than 25%. The experimental data shown in Fig. 5(a) were obtained with an angle of incidence  $\theta = 12.5^\circ$  and  $p$ -polarized radiation with the  $0.5 \text{ mm}$  sapphire delay plate. The amplitude and phase of the measured reflectance were fitted using the Drude model.<sup>10</sup> Figure 5(b) shows the dielectric function and conductivity calculated from the experimental data and those using the Drude model. The fits yield two independent parameters: the free-electron mobility  $\mu$  and concentration  $N_c$  (the dielectric constant of undoped silicon  $\epsilon_{\text{Si}} = 11.66$  is taken as a fixed value). From these values, the dc resistivity can be calculated using the formula  $\rho_{\text{dc}} = (\mu N_c e_0)^{-1}$ , where  $e_0$  is the elementary charge. One finds  $\mu = 1160 \text{ cm}^2/\text{V s}$ ,  $N_c = 4.0 \times 10^{16} \text{ cm}^{-3}$ , and  $\rho_{\text{dc}} = 0.135 \Omega \text{ cm}$  for the sample I and  $\mu = 1270 \text{ cm}^2/\text{V s}$ ,  $N_c = 2.8 \times 10^{16} \text{ cm}^{-3}$ , and  $\rho_{\text{dc}}$

$=0.175 \Omega \text{ cm}$  for the sample II. The values of the electron mobilities are consistent with those published previously for similar samples.<sup>8,10</sup> The dc resistivity values match the supplier's specifications.

## B. SBT ceramics

SBT is a promising material for application in ferroelectric memories and has been extensively investigated especially during the last few years. A study of IR reflectance revealed a rather strong polar phonon mode below  $30 \text{ cm}^{-1}$  at room temperature.<sup>13</sup> However, this frequency range is barely accessible for Fourier transform IR (FTIR) spectroscopy (the signal from the source is weak) and the measured power reflectance allows one to obtain the complex permittivity only by fitting with a model dielectric function. Therefore direct measurement of the complex permittivity can be useful for correction and improvement of FTIR data.

We have studied the reflectance of SBT ceramics using three different arrangements: (i)  $12.5^\circ$  incidence and  $p$  polarization, (ii)  $45^\circ$  incidence and  $p$  polarization, and (iii)  $45^\circ$  incidence and  $s$  polarization. The measured complex reflectance and calculated permittivity of SBT ceramics together with a fit of FTIR reflectance are presented in Fig. 6. From the fit we have found the soft-mode frequency  $\nu_0 = 28 \text{ cm}^{-1}$ , damping  $\gamma_0 = 12 \text{ cm}^{-1}$ , and dielectric strength  $\Delta\epsilon_0 = 81$ . It has to be pointed out that the peak in the relative phase which occurs near  $40 \text{ cm}^{-1}$  for SBT corresponds to the frequency of a longitudinal phonon mode, while the imaginary part of the permittivity (dielectric loss) peaks at the position of transverse resonance at  $\nu_0$ . One can see that TDTRS is able to reproduce correctly the mode structure at higher frequencies and brings valuable information down to at least  $10 \text{ cm}^{-1}$ . The complex permittivities measured in different arrangements are in agreement with each other, which demonstrates the reliability of the technique presented.

## C. SBT thin film

A  $5.5 \mu\text{m}$  thick SBT film on a (0001) sapphire substrate has been characterized in reflection as well as in transmission geometry. For the transmission measurements, the THz pulse transmitted through the bare sapphire substrate was used as a reference and the complex permittivity was numerically calculated in a standard way. The reflection measurement was performed using  $p$ -polarized THz pulses  $45^\circ$  incident on the sample with a blackened back surface to avoid the above-mentioned multiple reflection of the optical sampling beam inside the sapphire substrate (see Fig. 4). The complex reflectance was calculated taking into account only the THz pulse reflected from the front surface of the sample. Fabry-Pérot interference inside the substrate was cut off (time windowing). An additional correction was made to take into account multiple reflections of the sampling beam inside the film. Usually the thickness of thin films is smaller than  $1 \mu\text{m}$  and the delay of the sampling beam echoes is negligible compared to the duration of the sampling pulse (typically 50–100 fs). In our case (film thickness  $d = 5.5 \mu\text{m}$ ) special care has to be taken in order to deconvolute the influence of

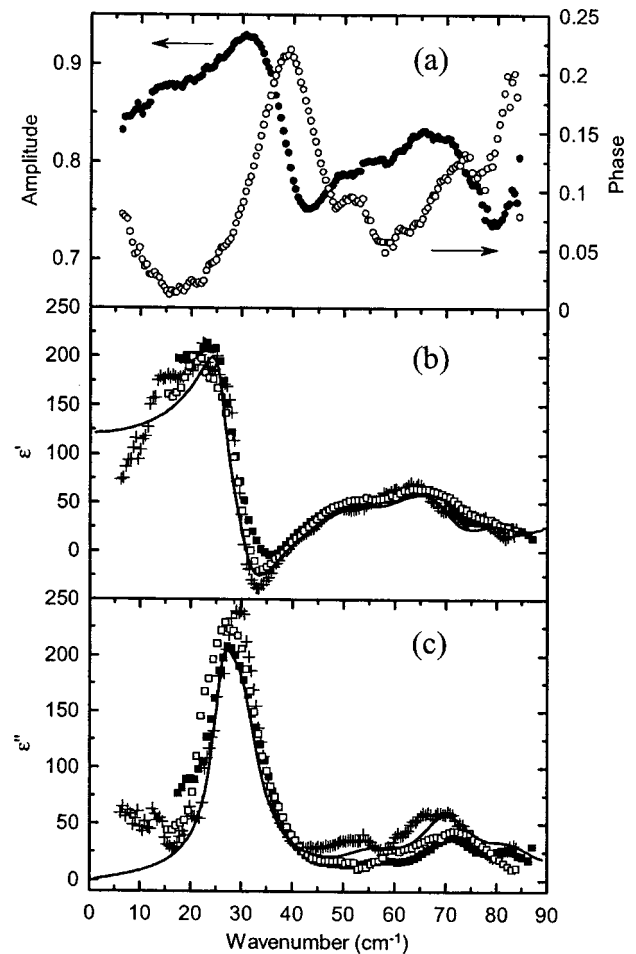


FIG. 6. Complex reflectance and dielectric permittivity of SBT ceramics from TDTRS measurements. (a) Complex reflectance for  $\theta=12.5^\circ$ ,  $p$  polarization; (●) amplitude; (○) phase. (b) Dielectric function; (c) dielectric loss; (+)  $\theta=12.5^\circ$ ,  $p$  polarization; (■)  $\theta=45^\circ$ ,  $p$  polarization, (□)  $\theta=45^\circ$ ,  $s$  polarization; solid lines: fit of the FTIR reflectance data based on the sum of damped harmonic oscillators.

Fabry-Pérot reflections of the sampling beam inside the film. The time delay of the sampling pulse needed for its propagation back and forth through the film can be calculated using Eq. (1). We deduced the optical refractive index of SBT from  $\epsilon_\infty$  obtained by FTIR measurements on SBT ceramics:  $n = 2.45$ ; the corresponding time delay is  $\Delta t = 94 \text{ fs}$ . Thus the sampling pulse is divided into a sequence of pulses with decreasing amplitude which are separated in time. The detected THz wave form can be written in the form of

$$y(t) = \frac{y_0(t) + ay_0(t + \Delta t) + \dots}{1 + a + \dots}, \quad (4)$$

where  $y_0(t)$  is the deconvoluted wave form (free of artifacts due to multiple reflections of the sampling beam), and  $a = 0.025$  is the ratio of the intensities of the first two sampling pulses calculated using Fresnel equations. The denominator of Eq. (4) accounts for normalization of the signal by the voltage of the reference photodiode. In view of the small value of  $a$ , all higher order terms in Eq. (4) can be neglected.

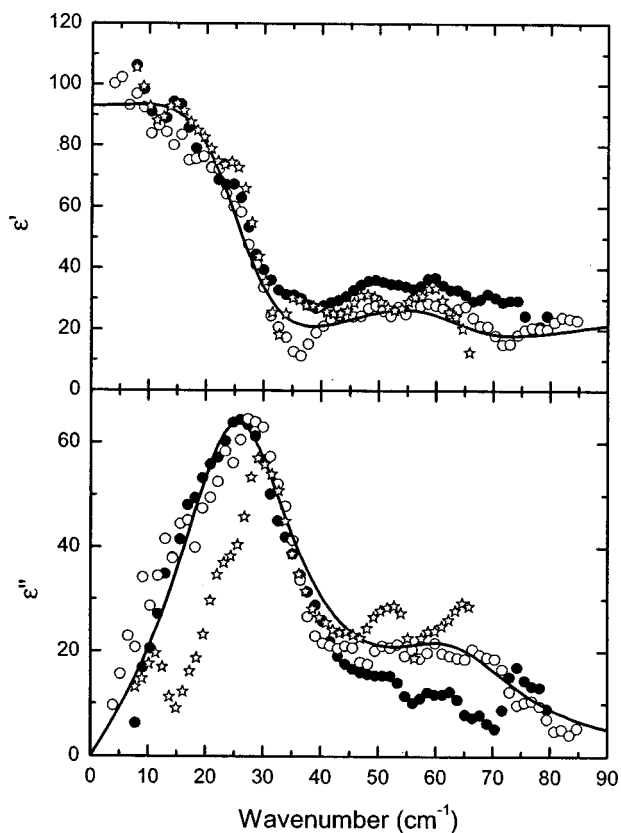


FIG. 7. Real and imaginary parts of the permittivity of the thin SBT film calculated by measurement of the complex transmittance (open circles), complex reflectance (solid circles,  $p$  polarization,  $\theta=45^\circ$ ), and amplitudes of the reflectance and transmittance (open stars). Solid lines correspond to the fit of the transmittance data.

Transforming Eq. (4) into the frequency domain and dividing it by the spectrum of the reference pulse we obtain for the complex reflectance

$$r_0(\omega) = r(\omega) \frac{1+a}{1+ae^{-i\omega\Delta t}}, \quad (5)$$

where  $r(\omega)$  is the measured reflectance and  $r_0(\omega)$  the corrected one which should be used for the evaluation of dielectric properties. This correction mainly leads to changes in the imaginary part of the permittivity. In the case of SBT film it increases the value of the dielectric loss peak by about 7%. The complex permittivity was calculated by numerically solving a system of two equations derived by Berreman<sup>14</sup> which relates the complex reflectance of a thin film on a substrate at an arbitrary angle of incidence to the dielectric constants of the thin film and substrate.

The resulting complex permittivity obtained from both transmission and reflection measurements and a fit of the transmission data by two damped harmonic oscillators are shown in Fig. 7. The fit yields the following parameters of the soft mode:  $\nu_0=28\text{ cm}^{-1}$ ,  $\gamma_0=26\text{ cm}^{-1}$ , and  $\Delta\epsilon_0=54$ . For comparison we also show the complex permittivity calculated from the amplitudes of the reflectance and transmittance (disregarding the respective phases). We would like to stress three points.

- (1) The transmission data can comprise large errors in the static value of the permittivity and in the strength of modes due to the uncertainty in substrate thickness.<sup>3</sup> In contrast, the substrate thickness does not play any role in the reflection experiment. Hence, one can use, e.g., the static value of the dielectric function determined by the reflection experiment for small corrections (within 1 or 2  $\mu\text{m}$ ) of the substrate thickness: trial substrate thicknesses can be used during the transmission data evaluation in order to match the resulting permittivity to that obtained from reflectance. Such an approach has been used to evaluate the transmission data shown in Fig. 7.
- (2) Evaluation of the complex permittivity using reflectance and transmittance amplitudes is indeed possible; moreover it does not require the value of the substrate thickness for transparent substrates. However, our experience shows that the results obtained by this method are not as accurate as the results of phase sensitive methods (note the appreciable error in the imaginary part of the permittivity in Fig. 7).
- (3) The data obtained from the transmission measurement using the above-described procedure fulfill slightly better the Kramers–Kronig relations than those obtained from the reflectance only. In this respect, if the substrate thickness is very precisely known, the transmission experiment seems to provide slightly more accurate data for this film. The transmission and reflection experiments are thus complementary in this sense and their combination allows unambiguous determination of the dielectric strength of the polar modes detected.

In summary, we have introduced a new approach for TDTRS which allows precise measurement of the dielectric function from reflectivity measurements. We have solved the key phase problem; as a result, the phase is independent of the relative position of the sample and reference mirror. This feature makes the method attractive also in situations where it is not possible to precisely align the sample holder, which is the case, e.g., in temperature-dependent measurements. We have shown that this method can be successfully applied to the characterization of a variety of materials.

## ACKNOWLEDGMENTS

This work was supported by the Ministry of Education of the Czech Republic (Project No. LN00A032), by the Grant Agency of the Czech Republic (Project No. 202/01/0612), and by the Volkswagen Stiftung (Grant No. I/75908).

<sup>1</sup> *Millimeter and Submillimeter Wave Spectroscopy of Solids*, edited by G. Grüner (Springer, Berlin, 1998).

<sup>2</sup> L. Duvillearet, F. Garet, and J.-L. Coutaz, *IEEE J. Quantum Electron.* **2**, 739 (1996).

<sup>3</sup> J. Petzelt, P. Kužel, I. Rychetský, A. Pashkin, and T. Ostapchuk, *Ferroelectrics* **288**, 169 (2003).

<sup>4</sup> S. C. Howells and L. A. Schlie, *Appl. Phys. Lett.* **69**, 550 (1996).

<sup>5</sup> L. Thrane, R. H. Jacobsen, P. U. Jepsen, and S. R. Keiding, *Chem. Phys. Lett.* **240**, 330 (1995).

<sup>6</sup> M. Khazan, R. Meissner, and I. Wilke, *Rev. Sci. Instrum.* **72**, 3427 (2001).

<sup>7</sup> T. Nagashima and M. Hangyo, *Appl. Phys. Lett.* **79**, 3917 (2001).

- <sup>8</sup>T.-I. Jeon and D. Grischowsky, *Appl. Phys. Lett.* **72**, 3032 (1998).
- <sup>9</sup>D. Hashimshony, I. Geltner, G. Cohen, Y. Avitzour, A. Zigler, and C. Smith, *J. Appl. Phys.* **90**, 5778 (2001).
- <sup>10</sup>S. Nashima, O. Morikawa, K. Takata, and M. Hangyo, *Appl. Phys. Lett.* **79**, 3923 (2001).
- <sup>11</sup>C. A. Paz de Araujo, J. E. Cuchiari, L. D. McMillan, M. C. Scott, and J. F. Scott, *Nature (London)* **374**, 627 (1995).
- <sup>12</sup>M. Li, G. C. Cho, T.-M. Lu, X.-C. Zhang, S.-Q. Wang, and J. T. Kennedy, *Appl. Phys. Lett.* **74**, 2113 (1999).
- <sup>13</sup>S. Kamba, J. Pokorný, V. Porokhonsky, J. Petzelt, M. P. Moret, A. Garg, Z. H. Barber, and R. Zallen, *Appl. Phys. Lett.* **81**, 1056 (2002).
- <sup>14</sup>D. W. Berreman, *Phys. Rev.* **130**, 2193 (1963).